

Na induced correlations in Na_xCoO_2

C. A. Marianetti¹ and G. Kotliar^{1,2,3}

¹*Department of Physics and Astronomy and Center for Condensed Matter Theory, Rutgers University, Piscataway, NJ 08854-8019*

²*Service de Physique Theorique, CEA Saclay, 91191 Gif-Sur-Yvette, France and*

³*Centre de Physique Theorique, Ecole Polytechnique 91128 Palaiseau Cedex, France*

(Dated: March 23, 2022)

Increasing experimental evidence is building which indicates that signatures of strong correlations are present in the Na rich region of Na_xCoO_2 (ie. $x \approx 0.7$) and absent in the Na poor region (ie. $x \approx 0.3$). This is unexpected given that NaCoO_2 is a band insulator and CoO_2 has an integer filled open shell making it a candidate for strong correlations. We explain these experimental observations by presenting a minimal low-energy Hamiltonian for the cobaltates and solving it within LDA+DMFT. The Na potential is shown to be a key element in understanding correlations in this material. Furthermore, LDA calculations for the realistic Na ordering predict a *binary* perturbation of the Co sites which correlates with the Na_1 sites (ie. Na sites above/below Co sites).

The qualitative features of the cobaltate phase diagram have been experimentally established [1]. Uncorrelated behavior is observed in the Na poor region while correlated behavior is observed in the Na rich region. For example, Magnetic susceptibility measurements show Pauli-like behavior for $x \approx 0.3$ and Curie-Weiss behavior for $x \approx 0.7$ [1] (for further references see [2]).

These observations are counterintuitive given our conventional understanding of Na_xCoO_2 . In NaCoO_2 , Co is in the 3+ configuration and thus has six electrons. The cubic component of the crystal field splits the d manifold into a set of 3-fold t_{2g} orbitals and 2-fold e_g orbitals, while the trigonal component will further split the t_{2g} orbitals into a_{1g} and e'_g . In this scenario, the six electrons of the Co will fill the t_{2g} orbitals (ie. $a_{1g} + e'_g$) resulting in a band insulator. On the contrary, in CoO_2 the Co will be in a 4+ configuration having 5 electrons in the t_{2g} shell, and may either be a metal or a Mott insulator.

There are two main puzzles posed by the above listed experimental observations. First, given that NaCoO_2 is a band insulator, it is difficult to understand why correlations are observed for the nearby composition of $x = 0.7$. The density of holes will be relatively low and therefore the on-site coulomb repulsion will have a minimal effect. Second, one would expect correlations to increase as the system is doped towards $x = 0.3$ as the hole density in the t_{2g} shell is increasing towards integer occupancy with an open shell. We resolve this puzzle by proposing a minimal low energy Hamiltonian which captures the essential physics and solve it within LDA+DMFT.

$$H = \sum_{ij\alpha\beta\sigma} t_{\alpha\beta} c_{i\alpha\sigma}^\dagger c_{j\beta\sigma} + \sum_{i\alpha\beta\sigma\sigma'} U_{\alpha\beta}^{\sigma\sigma'} n_{i\alpha\sigma} n_{i\beta\sigma'} + \sum_{i\alpha\sigma} \epsilon_{\alpha i} n_{\alpha i} (1 - \frac{x_1 \epsilon_1}{x_1 - 1})$$

where i, j are site indices, α, β are orbital indices running over a_{1g} and e'_g , t is the hopping parameter, U is the on-site Coulomb repulsions, and ϵ is the on-site potential which mimics the Na potential. It should be emphasized that the orbitals to which the creation operators refer

are low energy orbitals, effectively composed of oxygen p orbitals as well as Co d orbitals which compose the t_{2g} anti-bonding manifold. All the parameters of the Hamiltonian are in general functions of the total density, as the system rehybridizes [3] as a function of doping.

The hopping elements of the Hamiltonian are obtained using LDA calculations on NaCoO_2 and CoO_2 to be used for DMFT calculations in the Na rich region and Na poor region, respectively. The projected DOS for the a_{1g} and e'_g states are shown in figure 2 and 4, respectively. In both cases, the a_{1g} orbital has the overwhelming fraction of hole density. The doping dependence of the hopping parameters is substantial given the changes in the shape of the DOS and given that the total bandwidth increases by 0.25 eV for CoO_2 . Detailed cluster calculations for LiCoO_2 fit the on-site U to the experimental photoemission yielding $U = 3.5\text{eV}$ [4]. This should be very similar to NaCoO_2 , and we use a slightly reduced value of $U = 3\text{eV}$ because we are considering low-energy orbitals. Additionally, we assume U to be independent of doping. A nearest neighbor Coulomb interaction should be added to eq 1 in order to assist in forming charge ordered phases [5], and in single-site DMFT this results in a Hartree shift.

The on-site potential ϵ is treated as a *random binary* variable, and the fact that it is binary will be justified in the LDA calculations below. Treating the potential as random should be accurate for average quantities in the Na ordered phases, or even k-resolved quantities in the disordered region of the phase diagram. A fraction x_1 of the lattice sites will have a on-site potential ϵ_1 while $(1 - x_1)$ sites will have a on-site potential $\epsilon_2 = \frac{x_1 \epsilon_1}{x_1 - 1}$. We will assume that x_{ϵ_1} corresponds to $1 - x_{\text{Na}}$, where x_{Na} is the fraction of Na in the material. This also will be justified by our LDA calculations.

We propose that the Na potential plays a critical role in the behavior of this material. In a previous study of Li_xCoO_2 [3] (a very similar material), LDA calculations demonstrated that in the dilute Li-vacancy region of the

phase diagram, the Li vacancy binds the hole which is usually doped into the t_{2g} band and hence forms a half-filled impurity band split off from the valence band (analogous to Phosphorous doped Silicon, except the vacancies are highly mobile). Due to the fact that the impurity band is half-filled, it may be strongly correlated and form a Mott insulator if the on-site interaction is sufficiently strong. This behavior persists until enough holes are present to screen the Li vacancies upon which the more standard picture of doping into the t_{2g} states is recovered. The LDA calculations predict the impurity band to completely merge into the valence band once $x \approx 0.98$. Due to the similarities of the two materials, it is likely that a similar scenario occurs in Na_xCoO_2 . Of course, the experiments of interest are in a region of much higher doping (ie. $x \approx 0.7$) where it is implausible that an impurity band would persist. However, it is likely that the Na vacancies will still act as a strong perturbation towards the Co sites. Therefore, it is possible that the Na vacancy potential will cause certain Co sites to be higher in energy and possess a higher occupation than the average number of holes. Increasing the occupation of a given site towards integer filling will favor moment formation assuming that the on-site coulomb repulsion is sufficiently strong. This phenomena has been studied in detail in the context of model Hubbard Hamiltonians [6]. Merino et al. suggested a Hubbard model on a triangular lattice in the presence of an ordered potential in order to explain the correlated behavior observed in Na_xCoO_2 [7]. They note that in the limit of strong coupling of the ordered potential that correlations will be formed, similar to our work. NMR measurements strongly support this notion of certain Co sites being favored as there are distinct Co sites for $x = 0.7$ while there are not for $x = 0.3$ [8]. The fact that only one site is observed at $x = 0.3$ supports the notion that the Na potential is well screened and no longer a significant perturbation for small x .

In order to understand the effect of the Na potential described by the on-site potential ϵ in eq. 1, we performed LDA calculations on the $x = \frac{1}{3}$ and $x = \frac{3}{4}$ unit cells which were experimentally determined by Zandbergen et al [9]. These unit cells have 6 and 16 formula units for the $x = \frac{1}{3}$ and $x = \frac{3}{4}$ unit cells, respectively, and both contain equal numbers of occupied Na_1 and Na_2 sites. The Na_1 sites project directly onto the triangular Co lattice while the Na_2 sites project onto the centroids of the Co triangular lattice [9]. All LDA calculations were performed using the Vienna Ab-Initio Simulation Code (VASP) [10]. In order to quantify the effect of the Na potential on the different orbitals, the first moment $m_{i\alpha}$ of the projected DOS (ie. the on-site orbital energy) of the Oxygen and Cobalt orbitals are calculated for each site of the supercell. $m_{i\alpha} = \frac{\int \rho_{i\alpha}(\epsilon)\epsilon d\epsilon}{\int \rho_{i\alpha}(\epsilon) d\epsilon}$ where the indices i and α are the site and orbital indices, respectively. The deviation of the orbital energy from the site average is

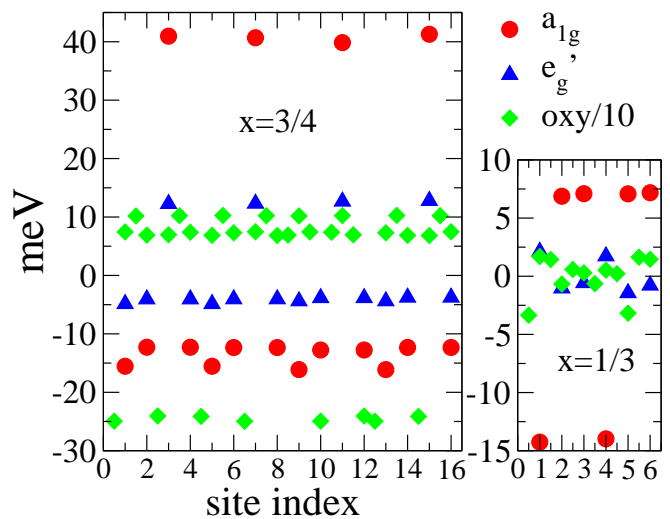


FIG. 1: The on-site orbital energy, $m_{i\alpha}$, relative to the average for various orbitals at each site in the unit cell. The energies for the oxygen orbitals have been divided by ten. The left and right panels correspond to $\text{Na}_{\frac{3}{4}}\text{CoO}_2$ and $\text{Na}_{\frac{1}{3}}\text{CoO}_2$, respectively.

shown in figure 1 (ie $m_{i\alpha} - \bar{m}_\alpha$). Remarkably, the results are roughly binary distributions as evidenced by the horizontal lines which are formed by the data points. The Na ordering causes each site to be perturbed, resulting in either a high or low energy orbital on a given site. The oxygen orbitals are perturbed the most followed by the a_{1g} and e'_g orbitals. The perturbations are substantially smaller for $x=\frac{1}{3}$ as compared to $x=\frac{3}{4}$, which is expected given that a larger amount of hole density is present at $x=\frac{1}{3}$ to screen the Na potential. A very simple rule governs the observed behavior. In the $x=\frac{3}{4}$ structure, all of the low energy a_{1g} and e'_g orbitals have one nearest-neighbor Na_1 present, while the high energy orbitals do not. There are 6 Na_1 sites occupied in this unit cell, each of which will have two Co nearest neighbors, and hence there are 4 high energy Co sites and 12 low energy sites. For the $x=\frac{1}{3}$ structure, the a_{1g} orbitals follow the same rule. However, the e'_g orbitals are perturbed in the opposite direction in this case. Although, the perturbations of the e'_g orbitals are all less than 2meV and should be considered carefully. The splitting of the oxygen orbitals also follow a simple rule in the $x=\frac{3}{4}$ structure. All of the low energy oxygens have three nearest-neighbor Na while the high energy oxygens only have two nearest-neighbor Na. For the $x=\frac{1}{3}$ structure, the oxygen do not split into a binary distribution, but it can be roughly understood as a ternary distribution if one analyzes both nearest and next-nearest neighbor Na. The low energy oxygen have three neighboring Na, the high energy oxygens have two Na_1 neighbors, while the intermediate energy oxygens have two Na_2 neighbors. Regardless, the a_{1g} and e'_g orbitals seem to depend only on the positions of the Na_1 .

This seems very reasonable for the a_{1g} orbitals given that they point directly towards the Na_1 sites (ie. $a_{1g} = d_{z^2}$ in the hexagonal coordinate system). This can be very important for several aspects of the low-energy behavior in this material. For example, this effect would tend to drive charge ordering to occur on the Co sites which are located directly above/below the occupied Na_1 sites. Additionally, this could effect the stabilization the pockets in the Fermi surface as the two orbitals are perturbed differently. For a recent study on the effect of Na on the Fermi surface see [11].

Obtaining parameters for a model Hamiltonian from LDA calculations is still an open problem. Therefore, we simply extract the qualitative effects of the Na potential. The binary splitting of the oxygen for $x = \frac{3}{4}$ is roughly 350 meV while for $x = \frac{1}{3}$ the maximum splitting is roughly 50 meV . This should be relevant to the low-energy Hamiltonian given that the hole density on the t_{2g} states has associated hole density on the oxygen via the rehybridization mechanism [3]. The changes on the Co are smaller, with the a_{1g} splitting being roughly 55 and 20 meV for $x = \frac{3}{4}$ and $x = \frac{1}{3}$, respectively. This is to be expected given that these states are near the Fermi energy and are not only well screened, but overscreened by LDA, and thus their bare values may be significantly larger. We take a value of $\epsilon_1 = 400 \text{ meV}$ for $x = \frac{3}{4}$ and $\epsilon_1 = \frac{400}{3} \text{ meV}$ for $x = \frac{1}{3}$, reflecting the fact that $x = \frac{1}{3}$ more screened. A more appropriate value for $x = \frac{1}{3}$ might be $\epsilon_1 = 0$ given that only a single Co is observed in NMR [8], and we explore this as well. We conservatively assume ϵ to be orbitally independent, which will make it more difficult to form correlations near the band insulator. Below we will demonstrate that these estimates yield predictions consistent with experimental observations.

With these order-of-magnitude estimates, we shall now proceed to solve the proposed Hamiltonian (equation 1) within LDA+DMFT [12], including the additional effect of binary disorder (see [13] for references). In this case there will be two impurity models which represent the two different binary environments. We begin with a guess for the average hybridization function Δ , and then construct the bath function $G_0 = (i\omega_n - E_{imp} + \mu - \Delta)^{-1}$ where E_{imp} is the average impurity level and μ is the chemical potential. We then construct the two disorder bath functions $G_0^{\epsilon_1} = (G_0^{-1} - \epsilon_1)^{-1}$ and $G_0^{\epsilon_2} = (G_0^{-1} - \epsilon_2)^{-1}$. The two corresponding impurity problems are then solved and the average Green's function is constructed as $G = x_{\epsilon_1} G_{\epsilon_1} + (1 - x_{\epsilon_1}) G_{\epsilon_2}$. The average self-energy is then constructed using Dyson's equation $\Sigma(i\omega_n) = G_0^{-1}(i\omega_n) - G^{-1}(i\omega_n)$. Finally, the DMFT self-consistency condition is performed:

$$G_0(i\omega_n) = \left[\Sigma(i\omega_n) + \left(\sum_k \frac{1}{i\omega_n - H_k + \mu - \Sigma(i\omega_n)} \right)^{-1} \right]^{-1} \quad (2)$$

where H_k is the homogeneous Hamiltonian (ie. eq.

1 with $\epsilon = 0$) in k -space. The entire process is then repeated until convergence is achieved. Given that the local Green's function is diagonal (ie. $a_{1g} + e'_g$), the summation over k in eqn. 2 can be replaced by a Hilbert transform (see [13]).

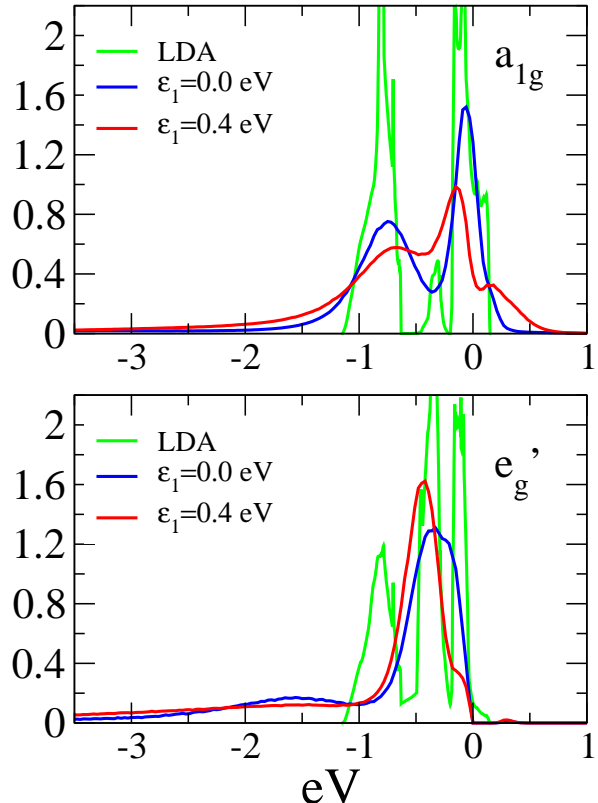


FIG. 2: Spectral functions for $\text{Na}_{0.7}\text{CoO}_2$ with random binary disorder for the a_{1g} and e'_g orbitals for $T=290 \text{ K}$.

The DMFT impurity problem is solved using Hirsch-Fye Quantum Monte-Carlo (see [12, 13]) using the LISA code [14]. All runs were performed with $\frac{\beta U}{T} = 1$ and 500,000 Monte-Carlo sweeps. We begin by considering the Na rich case of $x = 0.7$. The spectral functions for the a_{1g} orbital clearly shows the correlations increasing as the on-site potential is increased (Figure 2). The states at the Fermi energy are suppressed and spectral weight is transferred from low energies to higher energies as the on-site potential is increased. In both cases, the e'_g orbitals are pushed beneath the Fermi energy and the pockets are destroyed. Another useful quantity to analyze is the local magnetic susceptibility (see figure 3), which is one of the key experimental measurements. The susceptibility is relatively flat for the case with zero on-site potential, while a Curie-Weiss tail is clearly formed for the case when a on-site potential of 0.4 eV is included. In that latter case, 30% of the sites have 0.73 holes while 70% of the sites have 0.1 holes. This is qualitatively similar

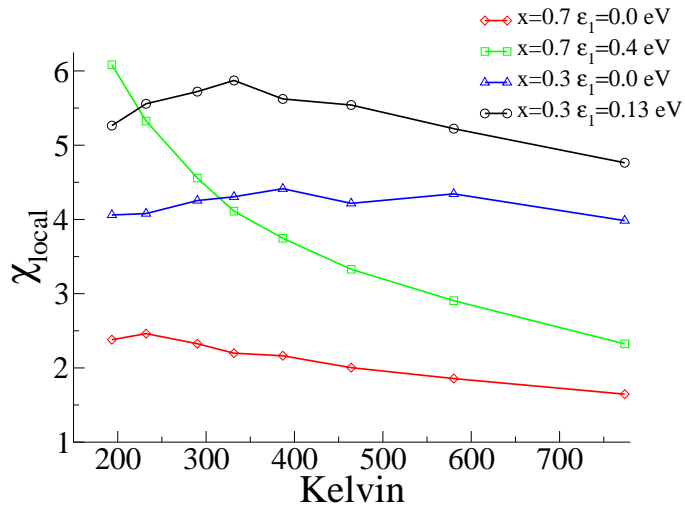


FIG. 3: Local Magnetic susceptibility versus temperature for Na_xCoO_2 .

to what is observed in NMR experiments [8]. Thus the ϵ_1 site becomes the favored site receiving significantly more hole density and being driven towards integer-filling where a local moment forms.

Now we proceed to the Na poor region and perform calculations at $x = \frac{1}{3}$. The spectral function for the a_{1g} orbital shows some indication of correlations as some spectral weight has been transferred to higher energies (see figure 4). Additionally, the e'_g orbitals show a small occupation in this case and the pockets survive as previously shown by Ishida et al [15]. The on-site potential only has a small effect on the spectral function. The main result is that the magnetic susceptibilities only shows a weak temperature dependence in both cases and there is no sign of a Curie-Weiss tail (see figure 3). The on-site potential clearly enhances the susceptibility but is not capable of building strong correlations. The on-site potential creates two distinct sites with 70% having 0.76 holes and 30% having 0.5 holes. Both susceptibilities cross the Curie tail of the $x = 0.7$ case in the vicinity of room temperature, similar to the crossover observed in experiment between 150-250 K [1].

An additional LDA+DMFT calculation for pure CoO_2 demonstrates that it is a strongly correlated metal with well formed Hubbard bands and a quasiparticle resonance at the Fermi energy. This guarantees that the susceptibility calculated for $\text{Na}_{0.3}\text{CoO}_2$ will not develop a Curie-Weiss tail at low temperatures which could not be reached in our QMC calculations.

In conclusion, we have proposed a low-energy Hamiltonian that is capable of explaining the observation of correlations near a band insulator and lack of correlation in the Na poor region of the doped cobaltates. Realistic parameters for the Hamiltonian obtained from LDA

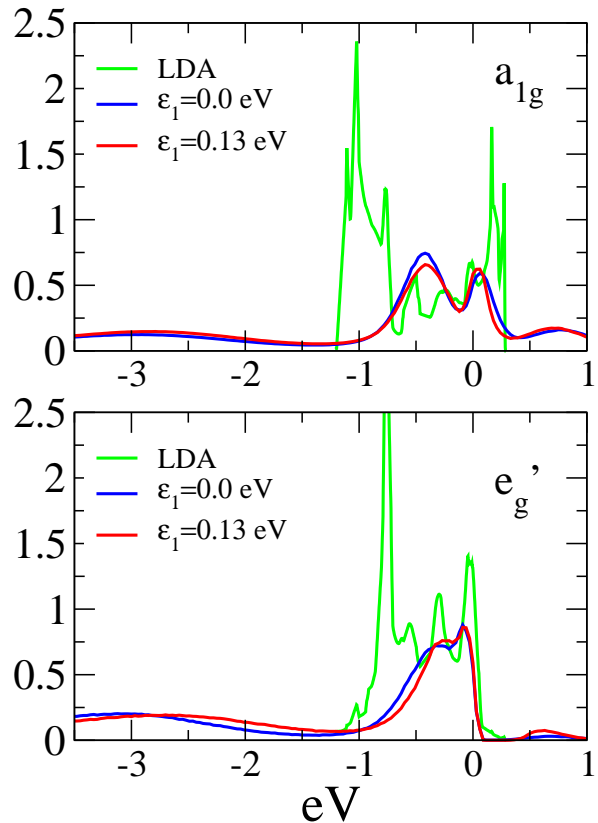


FIG. 4: Spectral functions at $\text{Na}_{0.3}\text{CoO}_2$ for the a_{1g} and e'_g orbitals for $T=290$ K.

calculations reproduce the generic behavior observed in the experimental magnetic susceptibility measurements. The Na potential is shown to be a key element in forming correlations near the band insulator. LDA calculations for the experimentally predicted Na orderings imply that the Na_1 sites act as a binary perturbing potential of the Co sites. Our model may be further improved by treating spatial correlation of the on-site potential, improved downfolding techniques to obtain the parameters of the low-energy Hamiltonian, inclusion of polarons, and the inclusion of the e_g states. The e_g states are needed to describe the high energy behavior of this system, and additionally may cause further renormalization at low energies. Including these effects may allow for significantly smaller values of the on-site potential ϵ in order to achieve the same qualitative effects.

-
- [1] M. L. Foo, Y. Y. Wang, S. Watauchi, H. W. Zandbergen, T. He, R. J. Cava, and N. P. Ong, Phys. Rev. Lett. **92**, 247001 (2004).
 - [2] Y. Ihara, K. Ishida, C. Michioka, M. Kato, K. Yoshimura, H. Sakurai, and E. Takayama-muromachi, J. Phys. Soc.

- Jpn. **73**, 2963 (2004).
- [3] C. A. Marianetti, G. Kotliar, and G. Ceder, Nature Materials **3**, 627 (2004).
- [4] J. Vanelp, J. L. Wieland, H. Eskes, P. Kuiper, G. A. Sawatzky, F. M. F. Degroot, and T. S. Turner, Phys. Rev. B **44**, 6090 (1991).
- [5] O. I. Motrunich and P. A. Lee, Phys. Rev. B **69**, 214516 (2004).
- [6] K. Byczuk, M. Ulmke, and D. Vollhardt, Phys. Rev. Lett. **90**, 196403 (2003).
- [7] J. . Merino, B. . J. . Powell, and R. . H. . Mckenzie, Cond-mat/0512696 (2005).
- [8] I. R. Mukhamedshin, H. Alloul, G. Collin, and N. Blanchard, Phys. Rev. Lett. **94**, 247602 (2005).
- [9] H. W. Zandbergen, M. Foo, Q. Xu, V. Kumar, and R. J. Cava, Phys. Rev. B **70**, 024101 (2004).
- [10] G. Kresse and J. Furthmuller, Phys. Rev. B **54**, 11169 (1996).
- [11] D. J. Singh and D. Kasinathan, Cond-mat/0604002 (2006).
- [12] G. Kotliar, S. Y. Savrasov, K. Haule, V. S. Oudovenko, O. Parcollet, and C. A. Marianetti, Cond-mat/0511085 (2006).
- [13] A. Georges, G. Kotliar, W. Krauth, and M. J. Rozenberg, Rev. Mod. Phys. **68**, 13 (1996).
- [14] O. Parcollet and C. A. Marianetti, <http://dmft.rutgers.edu> (2006).
- [15] H. Ishida, M. D. Johannes, and A. Liebsch, Phys. Rev. Lett. **94**, 196401 (2005).